BIOCHEMISTRY
including biophysical chemistry & molecular biology

Article

pubs.acs.org/biochemistry

Examination of ClpB Quaternary Structure and Linkage to Nucleotide Binding

JiaBei Lin and Aaron L. Lucius*

Department of Chemistry, The University of Alabama at Birmingham, 1530 Third Avenue S, Birmingham, Alabama 35294-1240, United States

Supporting Information

ABSTRACT: *Escherichia coli* caseinolytic peptidase B (ClpB) is a molecular chaperone with the unique ability to catalyze protein disaggregation in collaboration with the KJE system of chaperones. Like many AAA+ molecular motors, ClpB assembles into hexameric rings, and this reaction is thermodynamically linked to nucleotide binding. Here we show that ClpB exists in a dynamic equilibrium of monomers, dimers, tetramers, and hexamers in the presence of both limiting and excess ATPγS. We find that ClpB monomer is only able to bind one nucleotide, whereas all 12 sites in the hexameric ring are bound by nucleotide at saturating concentrations. Interestingly, dimers and tetramers exhibit stoichiometries of ∼3 and 7, respectively, which is one fewer than the maximum number of binding sites in the formed oligomer. This observation suggests an open conformation for the intermediates based on the need for an adjacent monomer to fully form the binding pocket. We also report the protein−protein interaction constants for dimers, tetramers, and hexamers and their dependencies on nucleotide. These interaction constants make it possible to predict the concentration of hexamers present and able to bind to cochaperones and polypeptide substrates. Such information is essential for the interpretation of many in vitro studies. Finally, the strategies presented here are broadly applicable to a large number of AAA+ molecular motors that assemble upon nucleotide binding and interact with partner proteins.

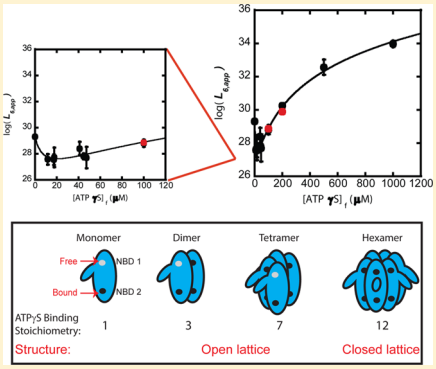

Escherichia coli caseinolytic peptidase B (ClpB) is a member of the Hsp100 protein family, a subfamily of the AAA+ (ATPase associated with various cellular activities) superfamily.[1] Hsp100 proteins play important roles in cell survival under stress including assisting protein folding and removing unfolded or misfolded proteins by degradation or remodeling.[2−6] *E. coli* ClpB and its eukaryotic orthologue; Hsp104 catalyze protein disaggregation in collaboration with cochaperones, DnaK (Hsp70).

Hsp100 proteins have been further classified as Class 1 or Class 2 members based on the presence of one or two nucleotide binding sites per monomer.[1] Both ClpA and ClpB are Class 1 members and contain two nucleotide binding sites per monomer. In contrast, ClpX contains one nucleotide binding site making it a Class 2 member. The role of the two nucleotide binding sites within Class 1 members is not fully understood.

ClpB is composed of an N-terminal domain followed by nucleotide binding domain 1 (D1) and domain 2 (D2).[1] Contained within D1 is a coiled-coil middle domain (m-domain) that is important for ClpB's function.[7] Mounting evidence suggests that the cochaperone, DnaK, binds the M-domain, and the interaction has an effect on ATP binding and hydrolysis.[8−11]

Many studies have shown that ClpB and the DnaK, DnaJ, and GrpE proteins (KJE) collaborate to catalyze protein disaggregation.[9,12] The phenomenological observation is that on model protein aggregates KJE or ClpB can catalyze some disaggregation. On the other hand, when the aggregate is exposed to both ClpB and KJE together the amount of disaggregation increases substantially more than the simple sum of their individual contributions. This observation has been described as a synergistic effect or a collaboration.[9,12−16] However, the molecular mechanism of this collaboration remains unclear. One possibility is that there is a direct protein−protein interaction between ClpB and DnaK.

Doyle et al. showed that a mixture of ATP and ATPγS could "unleash" the protein disaggregation activity catalyzed by ClpB/Hsp104 in the absence of the KJE cochaperones.[8] Further, they showed that a 3:1 and a 1:1 mixture of ATP:ATPγS could serve the same role as Hsp70/40 or KJE systems, for both Hsp104 and ClpB, respectively. This observation and a series of mutations in the nucleotide binding sites suggested that DnaK is influencing the nucleotide binding and/or hydrolysis function at either D1 or D2.

In an attempt to locate the position of the m-domain in cryo-EM experiments, Lee et al. engineered a chimera of Hsp104 containing T4 lysozyme in the m-domain.[17] In an unexpected result, similar to the mixture of ATP and ATPγS effect, this

Received: February 11, 2016
Revised: February 17, 2016
Published: February 18, 2016

DOI: 10.1021/acs.biochem.6b00122
Biochemistry 2016, 55, 1758−1771

construct was observed to have up-regulated disaggregation activity similar to what is observed in the presence of the cochaperone, Hsp70. Taken together these observations suggest that the cochaperone binds the m-domain, and this binding upregulates disaggregation activity through a complex interplay between the nucleotide ligation state, macromolecular assembly state, and the two enzymatic activities, ATPase and disaggregation.

More recent studies have definitively shown that DnaK interacts with the m-domain of ClpB. Using NMR titrations, Rosenzweig and co-workers showed, for the *T. thermophilus* system, that DnaK binds ClpB with an affinity of ~25 μM.[18] Moreover, they showed that residues within the m-domain were essential for this interaction.

The thermodynamic driving force for macromolecular assembly is the chemical potential of the monomer, i.e., the free monomer concentration. For a system like ClpB that requires nucleotide binding to assemble into an active hexamer, the thermodynamic driving force for assembly is both the chemical potential of the nucleotide and the protein. This thermodynamic fact predicts that a different population of hexamers will be present in solution depending upon the amount of both protein and nucleotide present in solution. For example, a different population of hexamers catalyzing ATP hydrolysis at each total [ATP] will be present in a determination of the steady state ATP hydrolysis rate collected at a fixed total protein concentration. Moreover, if DnaK does perturb the nucleotide ligation state, this, in turn, will perturb the assembly state.

Mogk and co-workers clearly showed that the steady state ATPase activity increased cooperatively with increasing *E. coli* ClpB concentration at a fixed ATP concentration of 2 mM.[19] This fundamentally indicates that changes in the macromolecular assembly state influence the observed steady-state ATP hydrolysis rate.

Many studies on Hsp104 and *Thermus thermophilus* ClpB have reported a cooperative increase in the ATPase activity as a function of ATP concentration to indicate cooperative interactions between the two ATP binding and hydrolysis sites.[7,20−25]Although one explanation for this observed cooperativity is, indeed, due to cooperativity between nucleotide binding sites, an equally viable explanation is changes in the macromolecular assembly state. On the basis of the work of Mogk et al., the latter is an equally likely explanation for *E. coli* ClpB.[19] However, both processes could be simultaneously occurring. Consequently, for a system like ClpB that exhibits nucleotide linked assembly, the observation of cooperativity in a steady-state ATPase experiment cannot be used to conclude only cooperativity between nucleotide binding sites. To address the question of cooperativity between sites one must deconvolute nucleotide binding from macromolecular assembly.

In vivo the ATP concentration is between 5 and 10 mM.[26,27] Thus, ClpB is likely saturated with nucleotide. However, the concentration of ClpB in vivo is ~9 μM at 37 °C but increases to ~20 μM during heat shock.[28] This suggests that, depending upon the hexamerization equilibrium constant, protein concentration may regulate ClpB hexamer formation. Moreover, if DnaK perturbs the nucleotide ligation state of ClpB when DnaK binds to ClpB, then this binding interaction will either stabilize or destabilize the hexamer. Thus, binding of partner proteins may also represent an in vivo regulatory mechanism for ClpB. To begin to address this question, a determination of the protein−protein interaction constants and their linkages to nucleotide binding is required. Only then can we begin to determine if the presence of DnaK perturbs the nucleotide ligation state which in turn will perturb the assembly state, which will influence the amount of motor present and available to do mechanical work.

Here we report a determination of the self-association equilibrium constants for *E. coli* ClpB and their functional dependencies on nucleotide concentration. The strength of this approach is that each self-association equilibrium constant as a function of nucleotide concentration represents a binding isotherm that represents binding to each oligomer in the absence of any changes in the oligomeric state. Consequently, we have deconvoluted macromolecular assembly from nucleotide binding. Strikingly, from a model independent thermodynamic analysis, we observe monomers, dimers, tetramers, and hexamers to bind 1, 3, 7, and 12 nucleotides, respectively, indicating that the hexamer exhibits full ligation and all smaller oligomers exhibit one fewer nucleotide bound per oligomer, i.e., partial saturation. This is in stark contrast to a recent model dependent ITC study that reported partial saturation for the hexamer.[29] The explanation for this is discussed below. Further, the binding isotherms for dimers, tetramers, and hexamers that have had the influence of macromolecular assembly removed exhibit no indication of cooperative interactions between the D1 and D2 binding sites. This is in agreement with our recently reported single-turnover polypeptide translocation experiments where the translocation rate constant as a function of [ATP] also did not exhibit any cooperativity.[30] It is important to note that, similar to the data presented here, the single turnover translocation rate constant as a function of [ATP] does not have any influence of macromolecular assembly since it only reflects the activity of the hexamer. These observations indicate that the previous reports of cooperativity in the steady state ATPase rates are likely due to changes in the assembly state and the interpretation needs to be revisited.

MATERIALS AND METHODS

Protein and Buffer. The 95 kDa *E. coli* ClpB was purified as previously described.[31] For the studies presented here it is important to note that we have taken care to ensure our protein sample is nucleotide free before adding ATPγS. On the basis of the primary structure of ClpB in 6 M guanidine the ratio of 260/280 nm absorbance has been calculated to be A_{260}/A_{280} = 0.66. Upon titrating purified ClpB into 6 M guanidine we have found an experimentally determined A_{260}/A_{280} = 0.67 ± 0.01, where the standard deviation is calculated from 10 replicates. This indicates that there is not a significant amount of contaminating nucleotide in the protein sample. Moreover, during the prep the protein is dialyzed several times against either 500 mM NaCl or 1 M NaCl in dialysis tubing above a 15 kDa cutoff. Absorbance spectra collected after each of these dialysis steps are also consistent with no significant contaminating nucleotide.

All experimental buffers were prepared with reagent grade chemicals using deionized H_2O produced using the Purelab Ultra Genetic system (EVOQUA Water Technologies). ATPγS was purchased from EMD biosciences and is 97% pure based on HPLC analysis. Buffer H200 contains 25 mM HEPES pH 7.5 at 25 °C, 10 mM $MgCl_2$, 2 mM 2-mercaptoethanol, 10% glycerol (v/v), and 200 mM NaCl.

Sedimentation Velocity Experiment Using Interference Optics. Interference sedimentation velocity experiments

DOI: 10.1021/acs.biochem.6b00122
Biochemistry 2016, 55, 1758−1771

were performed by using a Beckman ProteomeLab XL-I analytical ultracentrifuge. The experiments were carried out by loading 425 μL of the protein and 430 μL of the ATPγS reference sample into a double sector Epoxy charcoal-filled meniscus matching centerpiece. The sample was subjected to an angular velocity of 40 000 rpm. Interference scans were collected every 30 s at 25 °C.

Since interference is sensitive to the ATPγS concentration, a strategy to match the concentration of ATPγS in both the sample and reference sectors was developed. This was accomplished as follows. A stock concentration of ATPγS was prepared, and the concentration was determined by measuring the absorbance. From this stock, identical volumes were put into two separate Eppendorf tubes. The volume in each Eppendorf tube was verified by mass, and the mass difference between these two aliquots was found to be less than 1 mg (∼1 μL). A sample of ClpB with the concentration determined from absorbance measurements was added into one of the two Eppendorf tubes to make the protein sample containing ATPγS. ClpB dialysate (H200) of the identical volume as the protein was added into the other Eppendorf tube to make the ATPγS reference. Using this strategy, the ATPγS was diluted by the identical volume, and thus the two samples contained identical ATPγS concentrations. The dilution was further verified by mass.

The sample and reference solution for sedimentation velocity experiments were incubated at 25 °C for 2 h before the first interference scan was taken. Sedimentation velocity experiments on 2, 3, 6, and 10 μM ClpB in the presence of a fixed ATPγS concentration were performed in triplicate. Each experimental replicate was collected with freshly dialyzed ClpB samples no older than 3 days.

Sedimentation Velocity Experiment Using Absorbance Optics. Sedimentation velocity experiments using absorbance optics were carried out by loading a 380 μL sample of protein with ATPγS and 400 μL of protein dialysate (H200), as the reference, into a double sector centerpiece. Absorbance scans were taken at 230 or 260 nm as indicated in the text. The samples were mixed and incubated for 2 h before the first absorbance scan was collected. The sample was subjected to an angular velocity of 40 000 rpm, and absorbance scans were collected every 4 min at 25 °C.

Analysis of Sedimentation Velocity Data. REDATE (V. 0.1.7) was used to regenerate the sedimentation velocity data with corrected "elapse time" using the algorithm described by Zhao et al.[32] $c(s)$ analysis using SedFit[33] and time difference curve analysis using SedAnal[34] were used to fit sedimentation velocity data as previous described.[31]

The sedimentation coefficients used in SedAnal are not standardized to water solvent at 20 °C, $s_{20,w}$, and their values are constrained in the fits unless otherwise indicated. The sedimentation coefficient for ClpB monomer was obtained experimentally. A peak with sedimentation coefficient of s = (3.13 ± 0.06) S was observed in multiple $c(s)$ distributions when ATPγS is in large excess, where the error is the standard deviation of the mean value of three independent observations. The sedimentation coefficients for ClpB dimer (5.6 S), trimer (7.4 S), and tetramer (8.9 S) were calculated using WinHydroPro[35] as previously described.[31] In the presence of 1 mM ATPγS the hexameric state dominates the population. Thus, the ClpB hexamer sedimentation coefficient was obtained from global fitting of sedimentation velocity experiments for 2, 3, 6, and 10 μM ClpB in the presence of 1 mM ATPγS. The resulting s value for the hexamer is (11.11 ± 0.06) S. The error was calculated from the standard deviation of three experimental replicates. This value was then used and constrained as the hexamer sedimentation coefficient for all subsequent fits.

Sedimentation velocity data were analyzed between the meniscus plus 0.01 and 6.7 cm to minimize the effect of gradients of glycerol and ATPγS that can form during sedimentation. This range was chosen because the isosbestic point (radial position where all scans have the same absorbance/fringes) is shown to be at ∼6.7 cm for both glycerol[31] and ATPγS (see Figure S1). This indicates that the dominant effect of the formed gradient will occur at radial positions above 6.7 cm since ClpB (95 kDa) sediments much faster than either ATPγS (547 Da) or glycerol (92 Da).

Global Analysis of the Time Difference Curves from Sedimentation Velocity Experiments Performed at Various ClpB Concentrations for a Fixed ATPγS Concentration. Experiments performed with 2, 3, 6, and 10 μM ClpB in the presence of one fixed [ATPγS] (≥100 μM) were globally analyzed using SedAnal and the 1−2−4−6 model described in eqs 1−3,

$$2\{B_1\} \underset{k_{r2}}{\overset{k_{f2}}{\rightleftharpoons}} \{B_2\} \tag{1}$$

$$2\{B_2\} \underset{k_{r4}}{\overset{k_{f4}}{\rightleftharpoons}} \{B_4\} \tag{2}$$

$$\{B_2\} + \{B_4\} \underset{k_{r6}}{\overset{k_{f6}}{\rightleftharpoons}} \{B_6\} \tag{3}$$

where "$\{B_n\}$" represents ClpB n-mers at all ATPγS ligation states (including unligated). The stepwise equilibrium constants K_n for the formation of ClpB n-mer is related to the rate constants using eq 4.

$$K_n = \frac{k_{f,n}}{k_{r,n}} \tag{4}$$

K_n, $k_{r,n}$ and the loading concentrations of ClpB were set to float in the global analysis. The details on setting up the analysis can be found in refs 31 and ref 36.

Analysis of the Difference Curves from Sedimentation Velocity Data for a Single ClpB Concentration when the [ATPγS] Is Not in Large Excess over the [ClpB]. At a total [ATPγS] below 100 μM the free concentration, $[ATP\gamma S]_f$, cannot be assumed to be equal to the [ATPγS]t, $[ATP\gamma S]t$. Under these conditions, each sedimentation velocity experiment performed at a total [ClpB] = 2, 3, or 6 μM at a fixed $[ATP\gamma S]t$ < 100 μM were individually fit to the 1−2−4−6 model. The free [ATPγS] was experimentally determined for each sedimentation velocity experiment as described in Results.

Thermodynamic Reversibility Tests for ATPγS Linked ClpB Assembly. The ATPγS-linked ClpB assembly reaction was tested for thermodynamic reversibility and path independence. To address this, ATPγS was added to a large volume of ClpB to a final concentration of 3 μM ClpB and 500 μM ATPγS. The sample was incubated for 2 h at 25 °C. It was then diluted with a stock of 3 μM ClpB to a final concentration of 200 μM and 100 μM ATPγS. All volumes were confirmed by mass. The diluted samples were then incubated for another 4 h at 25 °C before the first sedimentation velocity interference scan was collected. The sedimentation velocity experiments

DOI: 10.1021/acs.biochem.6b00122
Biochemistry 2016, 55, 1758−1771

were performed as described above in the Sedimentation Velocity Experiment Using Interference Optics subsection. The data were analyzed as described in Analysis of the Difference Curves from Sedimentation Velocity Data for a Single ClpB Concentration subsection.

RESULTS

ClpB Exhibits Dynamic Assembly in the Presence of Nucleotide. We have shown that ClpB resides in a monomer, dimer, tetramer, and hexamer equilibrium in the absence of nucleotide.[31] To examine the impact of ATPγS binding on ClpB assembly, we performed sedimentation velocity experiments at 2 μM ClpB in the presence of (A) 0, (B) 200, and (C) 1000 μM ATPγS as described in Materials and Methods. The sedimentation boundaries were subjected to $c(s)$ analyses, and the results are shown in Figure 1 with the [ATPγS] indicated in the plots.

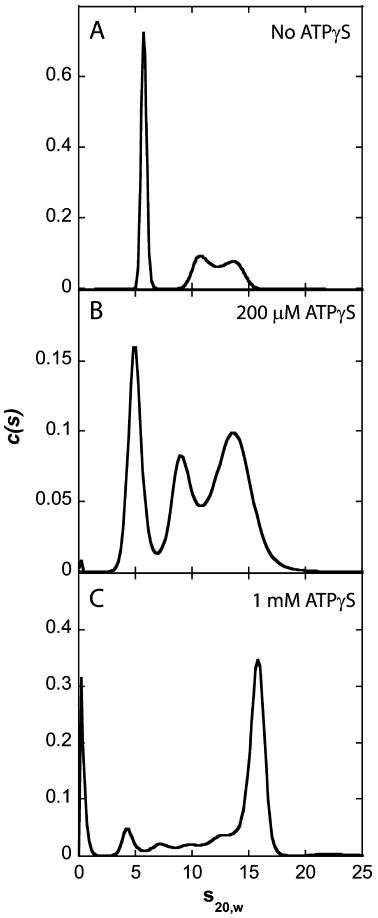

Figure 1. $c(s)$ analysis of sedimentation velocity data collected for ClpB in the presence of various concentrations of ATPγS. The $c(s)$ analysis from sedimentation velocity experiments performed as described in Materials and Methods with 2 μM ClpB in the presence of (A) no ATPγS, (B) 200 μM ATPγS, and (C) 1 mM ATPγS in Buffer H200.

Notably, in the absence of nucleotide (Figure 1A), multiple $c(s)$ peaks were observed, which we have reported to be the reaction boundaries for monomers, dimers, tetramers, and hexamers of ClpB.[31] When 200 μM ATPγS was added (Figure 1B), the overall weighted-average sedimentation coefficient, $\overline{s}_{20,w}$, shifts to larger values, from ∼8.7 S in the absence of ATPγS to ∼10.2 S. This indicates that the presence of ATPγS shifts the equilibrium toward higher order ClpB oligomers. Consistently, at 1 mM ATPγS, where the [ATPγS] is considered to be in large excess over the [ClpB], there is still a distribution of multiple $c(s)$ peaks but one peak at ∼15.5 S is predominant (Figure 1C). Under these conditions the weighted average sedimentation coefficient, $\overline{s}_{20,w}$ is increased to ∼13.6 S. Clearly, the presence of excess ATPγS shifts the equilibrium toward higher order oligomers of ClpB. As shown in Figure 1B,C, the assembly of ClpB in the presence of ATPγS is likely a dynamic process as observed for the assembly in the absence of nucleotide.[31]

ClpB Resides in a Monomer−Dimer−Tetramer−Hexamer Equilibrium in the Presence of ATPγS. To examine the linkage of ATPγS to ClpB assembly, we sought to determine the dependence of dimerization, tetramerization, and hexamerization on the concentration of ATPγS. To this end we examined ClpB assembly at multiple ClpB concentrations and multiple fixed ATPγS concentrations. Sedimentation velocity experiments at 2, 3, 6, and 10 μM ClpB at fixed $[\text{ATP}\gamma\text{S}]_t$ were performed to examine the apparent equilibrium constants, $L_{n,\text{app}}$, for the oligomerization of ClpB n-mer. $L_{n,\text{app}}$ as defined by eq 5,

$$L_{n,\text{app}} = L_{n,0}\frac{P_n}{(P_1)^n} \tag{5}$$

where $L_{n,0}$ is the stoichiometric equilibrium constant for ClpB n-merization in the absence of nucleotide, P_n is the partition function for ATPγS binding to ClpB n-mer, and P_1 is the partition function for ATPγS binding to ClpB monomer. The partition function, P_n, is a function of the free ATPγS concentration ($[\text{ATP}\gamma\text{S}]_f$), and it has no [ClpB] dependence.[37]

Sedimentation velocity experiments with 2, 3, 6, and 10 μM ClpB in the presence of 100, 200, 500 μM, or 1 mM ATPγS concentrations were performed using interference optics as described in Materials and Methods. The data collected from three experimental replicates were analyzed independently from the other replicates. Experimentally, when [ATPγS] is in large excess over the [ClpB], we consider $[\text{ATP}\gamma\text{S}]_f$ to be approximately equal to the total loading concentration. In this study we consider [ATPγS] of 100 μM, 200 μM, 500 μM, and 1 mM to be in large excess over [ClpB]. With this assumption in mind, the sedimentation velocity data at one fixed total [ATPγS] (e.g., 200 μM) with various ClpB concentrations were analyzed globally to obtain the stepwise assembly equilibrium constants, K_2, K_4, and K_6 defined in eqs 1−4 as shown in Materials and Methods. Figure S2 shows one example of the difference curves from a global analysis performed using the monomer, dimer, tetramer, hexamer model (1−2−4−6 model)[31] for 2, 3, 6, and 10 μM ClpB in the presence of a $[\text{ATP}\gamma\text{S}]_t$ of 200 μM.

The resulting stepwise equilibrium constants are converted to stoichiometric equilibrium constants, $L_{2,\text{app}}$, $L_{4,\text{app}}$, and $L_{6,\text{app}}$ using eqs 6−8. The averages and standard deviations from the three experimental replicates are reported in Table 1.

$$L_{2,\text{app}} = \frac{\{\text{B}_2\}}{\{\text{B}\}^2} = K_2 \tag{6}$$

$$L_{4,\text{app}} = \frac{\{\text{B}_4\}}{\{\text{B}\}^4} = K_2^2K_4 \tag{7}$$

DOI: 10.1021/acs.biochem.6b00122
Biochemistry 2016, 55, 1758−1771

$$L_{6,app} = \frac{\{B_6\}}{\{B\}^6} = K_2^3 K_4 K_6 \quad (8)$$

Table 1. Assembly Equilibrium Constants As a Function of $[ATP\gamma S]_f$

$[ATP\gamma S]_f$ (μM)	$\log(L_{2,app})$	$\log(L_{4,app})$	$\log(L_{6,app})$
0	5.24 ± 0.01	16.76 ± 0.03	29.30 ± 0.05
11.6 ± 0.5	4.9 ± 0.2	16.6 ± 0.1	27.6 ± 0.4
17.2 ± 0.3	5.1 ± 0.2	16.4 ± 0.2	27.5 ± 0.4
17.6 ± 0.2	5.2 ± 0.3	15.7 ± 0.7	27.7 ± 0.7
41.1 ± 0.2	5.2 ± 0.2	17.3 ± 0.3	28.4 ± 0.5
44.6 ± 0.6	4.5 ± 0.4	16.7 ± 0.3	27.8 ± 0.2
47 ± 1	4.6 ± 0.1	16.6 ± 0.2	27.7 ± 0.8
100	4.7 ± 0.4	17.3 ± 0.2	29.0 ± 0.2
200	4.7 ± 0.7	18.2 ± 0.1	30.2 ± 0.2
500	5.9 ± 0.2	19.5 ± 0.3	32.6 ± 0.5
1000	6.0 ± 0.3	20.1 ± 0.2	34.0 ± 0.2

The rate constant for dissociation of each oligomer, $k_{r,n}$, as defined by eqs 1−3 was floated as a fitting parameter for each $[ATP\gamma S]_f$. The average from the three experimental replicates together with the standard deviation are shown in Table 2.

Table 2. Dissociation Rate Constants As a Function of ATPγS

$[ATP\gamma S]_f$ (μM)	k_{r2} (s^{-1})	k_{r4} (s^{-1})	k_{r6} (s^{-1})
11.6 ± 0.5	3.7 ± 3.2	0.7 ± 0.7	3 ± 1
17.2 ± 0.3	9.9 ± 7.9	3.3 ± 4.7	4.9 ± 3.3
17.6 ± 0.2	0.48 ± 0.67	1.2 ± 0.9	1.3 ± 1.2
41.1 ± 0.2	1.4 ± 1.9	(5 ± 3) × 10^{-4}	5.3 ± 5.4
44.6 ± 0.6	3 ± 2	0.5 ± 0.6	4 ± 3
47 ± 1	9 ± 7	2.3 ± 1.7	2.6 ± 0.9
100	0.5 ± 0.6	0.2 ± 0.1	1.2 ± 1.4
200	2.4 ± 3.3	(8 ± 7) × 10^{-2}	(3 ± 1) × 10^{-3}
500	4 ± 3	(3.4 ± 2.9) × 10^{-5}	(2 ± 1) × 10^{-4}
1000	(6 ± 3) × 10^{-2}	(1 ± 0.7) × 10^{-5}	(5 ± 1) × 10^{-5}

At 100 μM ATPγS, the dissociation rate constants for dimer, tetramer, and hexamer are larger than 0.01 s^{-1}, which indicates that those oligomers undergo instantaneous dissociation on the time scale of sedimentation.

Notably, the rate constant for ClpB hexamer dissociation appears to exhibit an ATPγS concentration dependence. As the ATPγS concentration is increased from 100 μM to 200 μM, the dissociation rate constants decreased to (3 ± 1) × 10^{-3} s^{-1}. The dissociation rate constant is well constrained with a reasonably small standard deviation because rate constants in a range between ~10^{-2} and 10^{-5} s^{-1} are in the measurable range for sedimentation velocity experiments.[36] As the concentration of ATPγS is further increased, the dissociation rate constant for ClpB hexamer continues to decrease. This observation suggests that as the extent of binding of nucleotide to ClpB hexamer is increased, so is the kinetic stability.

Measurement of the Free ATPγS Concentration in Solution. For the experiments performed with 2, 3, or 6 μM ClpB in the presence of 20 μM or 50 μM ATPγS, respectively, the [ATPγS] are relatively low compared to the [ClpB]. Under these conditions the total ATPγS loading concentration, $[ATP\gamma S]_t$, cannot be considered to be equal to the free ATPγS concentration, $[ATP\gamma S]_f$. The $[ATP\gamma S]_f$ in solution will be different at each $[ClpB]_t$. Consequently, it is not possible to combine the sedimentation velocity data collected with 2, 3, and 6 μM ClpB in the presence of a total loading concentration of 20 or 50 μM ATPγS and subject the data to global NLLS analysis. Even though all three ClpB concentrations are examined at the same $[ATP\gamma S]_t$ each sample will contain a different $[ATP\gamma S]_f$ and thus a different ATPγS chemical potential.

To overcome this problem, we developed a sedimentation velocity strategy to determine the $[ATP\gamma S]_f$ at each $[ClpB]_t$ concentration for experiments performed with an $[ATP\gamma S]_t$ below 100 μM. We performed sedimentation velocity experiments as described above, but monitored absorbance at 260 nm. Figure 2A shows an example of absorbance scans from a sedimentation velocity experiment performed with 6 μM ClpB

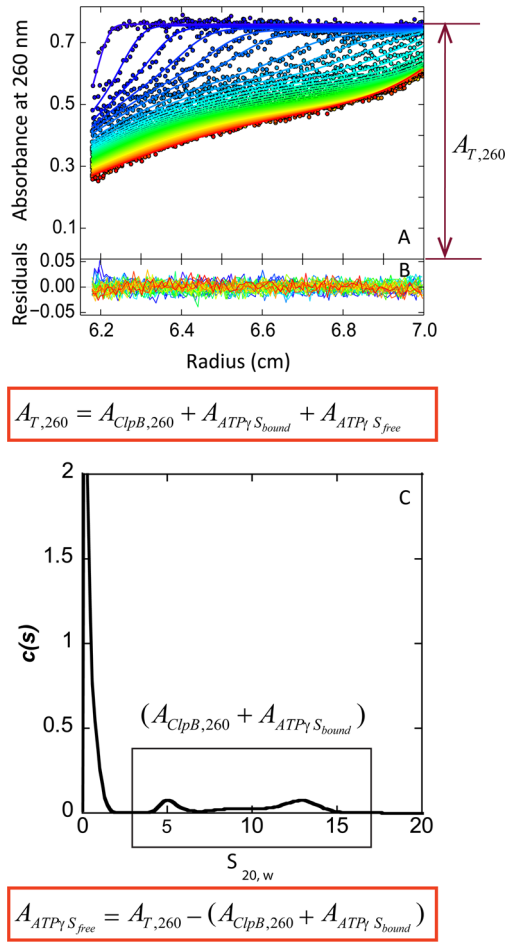

Figure 2. Sedimentation velocity experimental measurements of the free ATPγS concentration. $[ATP\gamma S]_f$ for ClpB assembly in the presence of 20 and 50 μM $[ATP\gamma S]_t$. (A) Sedimentation velocity experimental absorbance scans at 260 nm at 25 °C. The total observed absorbance is the summation of the absorbance for ClpB at 260 nm, the absorbance at 260 nm for the ATPγS bound to ClpB, and the absorbance at 260 nm for the unbound (free) ATPγS. The filled circles are data and solid lines are fits from the $c(s)$ analysis. (B) Residuals from the $c(s)$ analysis in panel A. (C) $c(s)$ as a function of $s_{20,w}$ from the analysis of sedimentation velocity data shown in panel A. The integrated area under the peaks represents the absorbance at 260 nm for the ClpB and the bound ATPγS. Thus, the difference between the total absorbance at 260 nm and the contribution of ClpB and the bound ATPγS yields the absorbance of the unbound ATPγS.

DOI: 10.1021/acs.biochem.6b00122
Biochemistry 2016, 55, 1758−1771

in the presence of 50 μM [ATPγS]$_t$. The scans were collected as described in Materials and Methods. At the beginning of the run, the total absorbance at 260 nm is a sum of the absorbance of three components: (1) ClpB absorbance at 260 nm, $A_{ClpB,260}$, ATPγS absorbance at 260 nm, which is composed of (2) ATPγS that is bound to ClpB, $A_{ATP\gamma S,bound}$, and (3) free ATPγS that is not bound by ClpB, $A_{ATP\gamma S,free}$.

When the centrifugal force is applied, ClpB and ClpB bound by ATPγS will sediment faster than the free ATPγS. Thus, the two components will be separated. The sedimentation boundaries shown in Figure 2A were subjected to $c(s)$ analysis. The observed $c(s)$ from 3.8 to 15.2 S (as shown in the black box of panel C) is considered to represent the absorbance at 260 nm for free ClpB and ATPγS bound by ClpB. Thus, the integrated area under the $c(s)$ curve from 3.8 to 15.2 S represents the contribution to the total absorbance signal of ClpB at 260 nm and ATPγS bound to ClpB. This contribution ($A_{ClpB,\ 260}$ + $A_{ATP\gamma S,bound}$) can be subtracted from the total absorbance at 260 nm, $A_{T,260}$, to yield the absorbance of the free ATPγS, $A_{ATP\gamma S,free}$. From this, [ATPγS]$_f$ is determined at each [ClpB]$_t$ and [ATPγS]$_t$.

These sedimentation velocity experiments were performed three times with 2, 3, and 6 μM ClpB at 20 and 50 μM total ATPγS. The average and standard deviation for each measured [ATPγS]$_f$ is reported in Table 1. The resulting $L_{2,app}$, $L_{4,app}$, and $L_{6,app}$ are reported in Table 1 for the corresponding [ATPγS]$_f$ determined as described in Materials and Methods.

Determination of the Binding Density of ClpB Oligomers. A model independent determination of the stoichiometry of nucleotide binding to each oligomer can be made using a Wyman plot.[38] This strategy has been previously discussed by Timasheff and others.[39,40] By taking the natural log of eq 5, we arrive at eq 9.

$$\ln(L_{n,app}) = \ln(L_{n,0}) + \ln(P_n) - n\ln(P_1) \quad (9)$$

Taking the first derivative of eq 9 with respect to ln[ATPγS]$_f$ yields eq 10.

$$\frac{\partial \ln(L_{n,app})}{\partial \ln[ATP\gamma S]_f} = \frac{\partial \ln(P_n)}{\partial \ln[ATP\gamma S]_f} - n\frac{\partial \ln(P_1)}{\partial \ln[ATP\gamma S]_f} \quad (10)$$

The derivative of the natural log of a partition function for binding with respect to the natural log of the ligand concentration is the extent of binding, $\bar{X}$ = [ligand bound]/[macromolecule]$_t$.[37] Thus, the two terms on the right-hand side of eq 10 represent the extent of binding to the n-mer ($\bar{X}_n$ = [ATPγS]$_b$/[ClpB$_n$]$_t$) and the extent of binding to the monomer ($\bar{X}_1$ = [ATPγS]$_b$/[ClpB$_1$]$_t$). Consequently, eq 10 tells us that the slope of the natural log of $L_{n,app}$ vs the natural log of the [ATPγS]$_f$ is equal to the difference between the extent of binding of nucleotide to the n-mer and n times the extent of binding to the monomer as given by eq 11.

$$\frac{\partial \ln(L_{n,app})}{\partial \ln[ATP\gamma S]_f} = \bar{X}_n - n\bar{X}_1 \quad (11)$$

With eq 11 in mind, the data in Table 1 were plotted as ln(L$_{n,app}$) vs ln([ATPγS]$_f$). The linear region of ln($L_{2,app}$), ln($L_{4,app}$) and ln($L_{6,app}$) as a function of ln[ATPγS]$_f$ were subjected to linear least-squares analysis using an equation for a line as shown in Figure 3. Notably, the linear regions of the Wyman plots were found to be at the high [ATPγS], which indicates that ClpB oligomers are likely approaching their maximum binding stoichiometry for ATPγS. Therefore, $\bar{X}_n$ can be a representation of the maximum binding stoichiometry of ClpB n-mer.[39] With the slopes determined from Figure 3, eq 11 can be written as

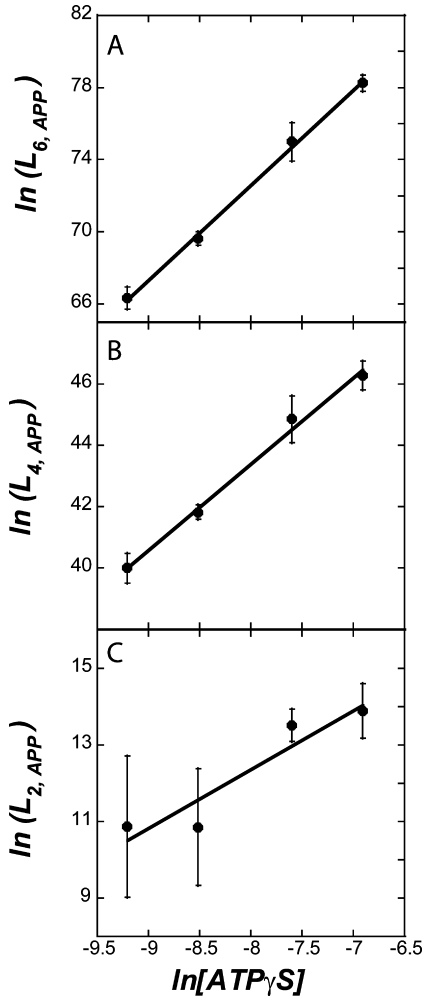

Figure 3. Log−log plot of the apparent self-association equilibrium constant vs [ATPγS]$_f$. (A) ln($L_{6,app}$), (B) ln($L_{4,app}$) and (C) ln($L_{2,app}$) as a function of ln[ATPγS]. The data are shown in black filled circles. A linear fit was applied to each plot. The slope and intercept for each line are (A) slope = 5.3 ± 0.2, intercept = 115 ± 1, (B) slope = 2.8 ± 0.2, intercept = 66 ± 1, and (C) slope = 1.5 ± 0.4, intercept = 25 ± 3.

$$\bar{X}_2 - 2\bar{X}_1 = 1.5 \pm 0.4 \quad (12)$$

$$\bar{X}_4 - 4\bar{X}_1 = 2.8 \pm 0.2 \quad (13)$$

$$\bar{X}_6 - 6\bar{X}_1 = 5.3 \pm 0.2 \quad (14)$$

Equations 12−14 represent a system of three linear equations with four unknowns. Thus, in order to solve eqs 12−14 for the binding stoichiometry to the dimer, tetramer, and hexamer we need to make assumptions about the binding of nucleotide to the monomer. Structurally we know that there are two nucleotide binding sites per ClpB monomer; therefore, we must have $\bar{X}_1 \leq 2$.

Solving the system of linear equations given by eqs 12−14 assuming that $\bar{X}_1$ is either 0, 1, or 2 yields the extent of binding for the other oligomers given in Table 3. If one assumes that both nucleotide binding sites are bound in the monomer, then Table 3 shows that the extent of binding to the dimers,

DOI: 10.1021/acs.biochem.6b00122
Biochemistry 2016, 55, 1758−1771

Table 3. Prediction for the Extent of Binding of ClpB Dimer $\bar{X}_2$, Tetramer $\bar{X}_4$ and Hexamer $\bar{X}_6$ Using the Slopes Determined from the Wyman Plots

	$\bar{X}_0 = 0$	$\bar{X}_1 = 1$	$\bar{X}_1 = 2$
$\bar{X}_2$	1.5 ± 0.4	3.5 ± 0.4	5.5 ± 0.4
$\bar{X}_4$	2.8 ± 0.2	6.8 ± 0.2	10.8 ± 0.2
$\bar{X}_6$	5.3 ± 0.2	11.3 ± 0.2	17.3 ± 0.2

tetramers, and hexamers is 5.5, 10.8, and 17.3, respectively. However, the dimer, tetramer, and hexamers have only 4, 8, and 12 binding sites, respectively. Because this analysis predicts a stoichiometry larger than the potential number of binding sites when both sites in the monomer are considered to be bound, we conclude that $\bar{X}_1$ cannot be equal to 2. Consistently, structural studies show that only one of the nucleotide binding sites in the monomer of ClpB is fully formed, and the other is fully formed with an arginine finger from an adjacent monomer upon oligomerization.[24] Thus, a partially ligated monomer is consistent with our knowledge of the structure.

Since a doubly ligated monomer is not likely, if we assume that the monomer does not bind or that the monomer binds one nucleotide, realistic numbers for the extent of binding to each oligomer are revealed; see Table 3. Thus, from this analysis we are left asking the question: does monomer bind only one nucleotide or none at all?

Global Analysis of $L_{n,app}$ Data As a Function of $[ATP\gamma S]_f$. To resolve the question of the stoichiometry and determine the nucleotide binding affinity to each oligomer, the

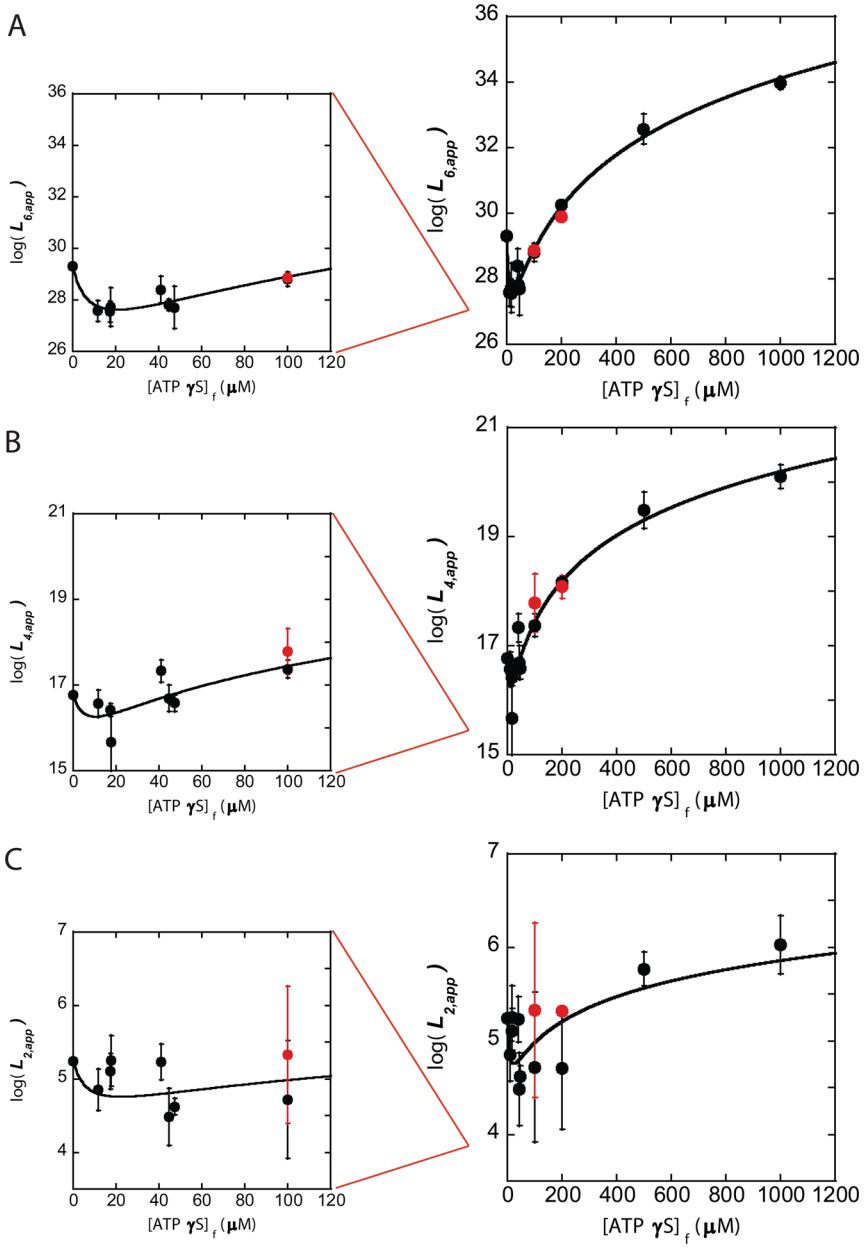

Figure 4. Global analysis of $L_{n,app}$. (A) Log($L_{6,app}$), (B) log($L_{4,app}$), and (C) log($L_{2,app}$)as a function of$[ATP\gamma S]_f$. Left panel is a zoom-in of the 0−120 μM $[ATP\gamma S]_f$ region of the right panel. The black filled circles are the results from the analysis of the sedimentation velocity data presented in Table 1. The solid lines are the results from a global NLLS analysis using eqs 19−21 with log($L_{2,0}$) = 5.24, log($L_{4,0}$) = 16.76 log($L_{6,0}$) = 29.30, m_1 = 1, m_2 = 3, m_4 = 7, m_6 = 12 and the best fit values for the nucleotide binding constants κ_1, κ_2, κ_4, and κ_6 are given in Table 4.

DOI: 10.1021/acs.biochem.6b00122
Biochemistry 2016, 55, 1758−1771

equilibrium constants in Table 1 are plotted in Figure 4. For all three equilibrium constants, the value is observed to decrease at low ATPγS concentration. Above ~50 μM ATPγS, the value is observed to increase.

Equation 5 shows that $L_{n,app}$ is a function of the partition functions for nucleotide binding to the n-mer and the monomer. Thus, to analyze the plots shown in Figure 4A−C one must define a partition function for nucleotide binding to each oligomer. The simplest way to describe nucleotide binding to each of the sites in a ClpB oligomer is to assume that they are identical and independent, i.e., no cooperativity. Thus, the n-independent and identical sites model was used to examine the data. Equation 15 is the partition function for the n-independent and identical sites model.

$$p_n = (1 + \kappa_n[\mathrm{ATP}\gamma\mathrm{S}]_f)^{m_n} \quad (15)$$

where κ_n represents the average stepwise equilibrium constant for binding to an n-mer and m_n is the number of binding sites in an n-mer.[37]

The partition function for nucleotide binding to each oligomer, given by eq 15, is substituted into eq 5 to yield eqs 16−18.

$$L_{2,app} = L_{2,0}\frac{(1 + \kappa_2[\mathrm{ATP}\gamma\mathrm{S}]_f)^{m_2}}{((1 + \kappa_1[\mathrm{ATP}\gamma\mathrm{S}]_f)^{m_1})^2} \quad (16)$$

$$L_{4,app} = L_{4,0}\frac{(1 + \kappa_4[\mathrm{ATP}\gamma\mathrm{S}]_f)^{m_4}}{((1 + \kappa_1[\mathrm{ATP}\gamma\mathrm{S}]_f)^{m_1})^4} \quad (17)$$

$$L_{6,app} = L_{6,0}\frac{(1 + \kappa_6[\mathrm{ATP}\gamma\mathrm{S}]_f)^{m_6}}{((1 + \kappa_1[\mathrm{ATP}\gamma\mathrm{S}]_f)^{m_1})^6} \quad (18)$$

where $L_{2,0}$, $L_{4,0}$, and $L_{6,0}$ represent dimerization, tetramerization, and hexamerization in the absence of nucleotide and have been previously reported by us in these solution conditions,[31] κ_1, κ_2, κ_4, and κ_6 are the average stepwise equilibrium constants for nucleotide binding, m_1, m_2, m_4, and m_6 are the stoichiometries of binding to monomers, dimers, tetramers, and hexamers, respectively.

The data in Figure 4 were subjected to global NLLS analysis using the logarithmic form of eqs 16−18 given by eqs 19−21.

$$\log(L_{2,app}) = \log(L_{2,0}) + \log(1 + \kappa_2[\mathrm{ATP}\gamma\mathrm{S}]_f)^{m_2} - 2\log(1 + \kappa_1[\mathrm{ATP}\gamma\mathrm{S}]_f)^{m_1} \quad (19)$$

$$\log(L_{4,app}) = \log(L_{4,0}) + \log(1 + \kappa_4[\mathrm{ATP}\gamma\mathrm{S}]_f)^{m_4} - 4\log(1 + \kappa_1[\mathrm{ATP}\gamma\mathrm{S}]_f)^{m_1} \quad (20)$$

$$\log(L_{6,app}) = \log(L_{6,0}) + \log(1 + \kappa_6[\mathrm{ATP}\gamma\mathrm{S}]_f)^{m_6} - 6\log(1 + \kappa_1[\mathrm{ATP}\gamma\mathrm{S}]_f)^{m_1} \quad (21)$$

In this analysis, κ_1 and m_1 are global parameters, $\log(L_{2,0})$, $\log(L_{4,0})$, and $\log(L_{6,0})$ are constrained to our previously reported values shown in Table 1, κ_2, κ_4, κ_6, and m_2, m_4, and m_6 are local parameters and are allowed to float in the analysis. As discussed above, we have ruled out the possibility of two nucleotides binding to the monomer, $m_1 \neq 2$. Thus, we are left with $m_1 = 0$ or 1. However, if $m_1 = 0$ then the denominators in eqs 16−18 collapse to 1 and the system of equations will not describe the decreasing equilibrium constant exhibited in Figure 4A,B at low ATPγS concentrations. Consistently, when the data were subjected to NLLS analysis using eqs 19−21 with $m_1 = 0$ the fit always has positive slope and the data are not well described (see Figure S3).

When $m_1 = 1$, both κ_n and m_n floated to the values shown in Table 4 and the fits are able to describe both the descending and ascending regions in the isotherms (see solid lines in Figure 4A−C). Most importantly, the values of the stoichiometries from the fitting are within error of the values determined from the model independent Wyman analysis; compare stoichiometries in the first column of Table 4 to extent of binding values in Table 3 when the monomer is assumed to bind only one nucleotide. Thus, the fit was redone by constraining the stoichiometries to 1, 3, 7, and 12 for the monomer, dimer, tetramer, and hexamer, respectively. The result of this analysis yields a slightly improved variance and the resultant binding constants are given in Table 4.

Table 4. ATPγS Binding Constants and Binding Stoichiometry Determined from Global Analysis of log $L_{n,app}$ as a Function of $[\mathrm{ATP}\gamma\mathrm{S}]_f$

floating parameters	with m_n floating variance = 2.55×10^{-3}	with m_n constrained variance = 2.53×10^{-3}
κ_1 (M^{-1})	$(2.9 \pm 0.5) \times 10^5$	$(2.0 \pm 0.3) \times 10^5$
κ_2 (M^{-1})	$(6 \pm 1) \times 10^4$	$(6 \pm 1) \times 10^4$
κ_4 (M^{-1})	$(1 \pm 0.1) \times 10^5$	$(6.7 \pm 0.7) \times 10^4$
κ_6 (M^{-1})	$(4.6 \pm 0.7) \times 10^4$	$(3.6 \pm 0.4) \times 10^4$
m_1	1*	1*
m_2	3.2 ± 0.3	3*
m_4	6.5 ± 0.3	7*
m_6	11.6 ± 0.5	12*

With the stoichiometries constrained, the binding isotherms shown in Figure 4A−C are being described by one local parameter and one globally optimized parameter. Nevertheless, we asked the question: how well constrained are these parameters and what degree of correlation do they exhibit? To address this question we performed a grid search on each parameter. The results of the grid search are shown in Figure S4, and they clearly indicate that the parameters are well constrained.

The next level of complexity would be to include cooperativity between binding sites. However, the data do not suggest that any cooperativity is present; i.e., the isotherms are not sufficiently steep to suggest cooperativity. Moreover, because of the quality of the fit to the n-independent and identical sites model, there is no justification for fitting the data to a more complex model. Nevertheless, the data were subjected to NLLS analysis using a fully cooperative nucleotide binding model, i.e., Hill model. The fits using this model are statistically worse than the n-independent and identical sites model and are shown in Figure S5. As expected, the fully cooperative model predicts that the descending and ascending regions of the plot are much more steep than we experimentally observe; see Figure S5.

ClpB Monomer Binds ATPγS. One might ask: is the observed decreasing self-association equilibrium constant between zero and ~50 μM $[\mathrm{ATP}\gamma\mathrm{S}]_f$ statistically significant? As seen in Table 1 and Figure 4, the values of the equilibrium constants between zero and ~50 μM are not within error. However, the observation that the equilibrium constants decrease is surprising. Nevertheless, direct experimental evidence was acquired that supports this observation. Figure

DOI: 10.1021/acs.biochem.6b00122
Biochemistry 2016, 55, 1758−1771

5 shows a $c(s)$ plot for 2 μM ClpB in the presence and absence of 10 μM [ATPγS]$_t$. Strikingly, in the absence of nucleotide, we

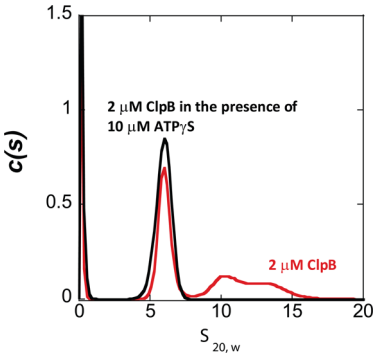

Figure 5. $c(s)$ distributions for sedimentation velocity experiments performed with 2 μM ClpB in the absence (red curve) or presence of 10 μM [ATPγS]$_t$(black curve). The scans were collected and subjected to $c(s)$ analysis as described in Materials and Methods.

observe a distribution of monomers and higher order oligomers. However, upon addition of 10 μM ATPγS the $c(s)$ distribution does not exhibit any higher order oligomers and only monomers are present. Thus, binding of nucleotide at low concentration appears to disrupt the oligomers that form in the absence of nucleotide. We interpret this to be direct evidence of nucleotide binding to the monomer.

ATPγS Driven ClpB Assembly Reaction Is Thermodynamically Reversible. The nucleotide driven assembly reaction was tested for thermodynamic reversibility. All of the experiments reported above were performed by adding ATPγS to ClpB. Thus, the sample proceeds from zero ATPγS to some final ATPγS concentration. To test for reversibility 500 μM ATPγS was added to a sample of ClpB at a final concentration of 3 μM. This sample was allowed to incubate for 2 h. After the incubation, 3 μM ClpB was added to dilute the sample to either 200 or 100 μM total ATPγS. The sample was examined by sedimentation velocity experiments and the equilibrium constants for dimers, tetramers, and hexamers were determined as described. As shown in Figure 4, the equilibrium constants obtained from diluting the sample from a high concentration of ATPγS to 200 or 100 μM ATPγS (red filled circles) agree with the equilibrium constants obtained when going from no ATPγS to 200 or 100 μM ATPγS (black filled circles). This indicates that the ATPγS-linked ClpB assembly reactions are both thermodynamically reversible and path independent.

Importantly, it has been reported that ClpB hydrolyzes ATPγS with a $k_{cat} \approx 0.2$ min^{-1} (M hexamer)$^{-1}$. Our observation that the assembly reaction is thermodynamically reversible indicates that the production of ADP due to ATPγS hydrolysis does not significantly affect the assembly reaction. This is because the test for reversibility results in exposing the ATPγS to ClpB for an additional 4 h compared to all other experiments reported here, which only use a 2 h incubation time (see Materials and Methods). Thus, if ATPγS hydrolysis produces a significant amount of ADP then the additional ADP produced in four more hours of incubation does not significantly perturb the equilibrium.

DISCUSSION

Class 1 AAA+ molecular chaperones like ClpA, ClpB, ClpC,[41] Hsp104,[42] NSF,[43] VCP/p97,[44] and many others contain two ATPases per monomer unit.[1] The consequence of this, for ClpA and ClpB, is that the active hexamer contains 12 nucleotide binding sites. However, there are many hexameric ring motors that perform their mechanical work with only six sites per hexamer. For example, ClpA and ClpX can both associate with the same protease, ClpP.[45,46] Both motors couple the energy from ATP binding and hydrolysis to translocate a substrate into ClpP for proteolytic degradation. So the question is why does ClpA require two ATP binding sites per monomer, whereas ClpX only requires one to perform the same mechanical work?

One common feature among many Class 1 and Class 2 members is that the motors often operate with partner proteins.[1] Examples of partner proteins include proteases, adaptor proteins, and cochaperones. We hypothesize that interactions with partner proteins modulates the stoichiometry and/or the binding affinity for nucleotide. As shown in this work, any changes in the affinity or ligation state of the nucleotide will change the hexamerization equilibrium constant ($L_{6,app}$) and thereby shift the population of hexamers present and able to perform catalysis. Thus, binding of partner proteins and changing the nucleotide ligation state may represent an unexplored mechanism by which partner proteins regulate the activity of the motor.

One example supporting the idea that partner proteins modulate the nucleotide ligation state comes from our recent studies on ClpA and ClpAP. We examined ClpA catalyzed polypeptide translocation and showed that the elementary translocation rate constant exhibited a sigmoidal dependence on [ATP] and saturated in less than one log unit in concentration.[47] These observations indicate that ATP is binding cooperatively, for which there are three possible explanations: (1) intramolecular communication between D1 and D2 within a monomer, (2) intermolecular communication between sites in adjacent subunits, or (3) changes in the macromolecular assembly state with [ATP]. Those experiments were single-turnover with respect to the polypeptide substrate with ClpA prebound to the polypeptide substrate. Consequently, the signal reflects a single translocation cycle catalyzed by only the hexamer. Therefore, changes in the macromolecular assembly state can be ruled out since, under these single-turnover conditions, the signal is sensitive to the events in the active site of only the hexamer.[48] Thus, for ClpA alone, the observed cooperativity indicates that there is either intra- or intermolecular communication between ATP binding sites during polypeptide translocation.

In stark contrast to our observations with ClpA alone, when ClpP was bound to ClpA, the observed cooperative dependence on [ATP] was no longer present. This indicated that the presence of the protease influenced how the molecular motor was coordinating its use of the two ATP binding and hydrolysis sites during polypeptide translocation.[49]

We recently reported the same type of single turnover polypeptide translocation experiments for *E. coli* ClpB. In addition to showing that ClpB is a nonprocessive translocase, we showed that ClpB dissociated from the polypeptide in two rate limiting steps. Both steps were found to depend on [ATP]. However, these two rate-limiting steps did not exhibit any cooperative dependence on [ATP].[30] Consistent with our previous report,[30] we report here that there is no apparent cooperativity in the dependence of the self-association equilibrium constants, $L_{n,app}$ on [ATPγS].

DOI: 10.1021/acs.biochem.6b00122
Biochemistry 2016, 55, 1758−1771

Many studies on Hsp104 and *T. thermophilus* ClpB have reported a cooperative increase in the steady-state ATPase rate as a function of ATP concentration. This observation has been used to conclude that there are cooperative interactions between the two ATP binding and hydrolysis sites.[7,20−25] However, in a steady-state ATPase experiment, all species that hydrolyze ATP will contribute to the signal. Moreover, changes in the macromolecular assembly with increasing ATP concentration can also give rise to a sigmoidal dependence on [ATP].

Here we have shown that *E. coli* ClpB exists in a dynamic equilibrium of monomers, dimers, tetramers, and hexamers, and the population of each oligomer depends on nucleotide concentration. Therefore, a determination of a steady-state rate at a fixed [ATP] will reflect the summation of the rate of hydrolysis catalyzed by monomers, dimers, tetramers, and hexamers if all of the oligomers hydrolyze ATP. The total rate of ATP hydrolysis, v_{obs}, can be easily modeled by the following equation.

$$v_{obs} = v_1 f_{mon} + v_2 f_{dim} + v_4 f_{tet} + v_6 f_{hex} \quad (22)$$

where v_{obs} is the observed rate at a fixed ATP concentration, v_1, v_2, v_4, and v_6 are the steady-state ATPase rates for the monomers, dimers, tetramers, and hexamers, respectively, and f_{mon}, f_{dim}, f_{tet}, and f_{hex} are the fractional populations of monomers, dimers tetramers and hexamers, respectively, given by eqs 23−26.

$$f_{mon} = \frac{[ClpB]_f(1 + \kappa_1[ATP]_f)^{n_1}}{[ClpB]_{total}} \quad (23)$$

$$f_{dim} = \frac{2[ClpB]_f^2 L_{2,0}(1 + \kappa_2[ATP]_f)^{n_2}}{[ClpB]_{total}} \quad (24)$$

$$f_{tet} = \frac{4[ClpB]_f^4 L_{4,0}(1 + \kappa_4[ATP]_f)^{n_4}}{[ClpB]_{total}} \quad (25)$$

$$f_{hex} = \frac{6[ClpB]_f^6 L_{6,0}(1 + \kappa_6[ATP]_f)^{n_6}}{[ClpB]_{total}} \quad (26)$$

Figure 6 is a simulation using eqs 23−26 and the nucleotide binding constants and stoichiometries in Table 4 and the $L_{n,0}$ values for the solution conditions used here and published in Lin and Lucius.[31] The total ClpB concentration was considered to be 5 μM and the range of ATP was 30 μM to 1 mM. The ATP and ClpB concentrations were chosen because they represent the concentrations used in Schlee et al. where it was reported that the steady state rate depends sigmoidally on [ATP] for *T. thermophilus* ClpB.[20]

It is important to note that eqs 23−26 assume there is no cooperativity between nucleotide binding sites. Nevertheless, the simulation exhibited in Figure 6 reveal that the hexameric species concentration is decreasing at low [ATP] and then increases with increasing [ATP]. If only the hexamer were hydrolyzing ATP then eq 22 would collapse to $v_{obs} = v_6 f_{hex}$. Thus, the observed ATP hydrolysis plot would be given by the solid black line in Figure 6 scaled by the rate of ATP hydrolysis, v_6, catalyzed by the hexamer. Although a slight decrease in population is observed at low [ATP], with experimental uncertainty, this plot would likely appear sigmoidal. On the other hand, other oligomers are likely also hydrolyzing ATP, and, as given by eq 22, the observed rate, v_{obs}, would be the summation of each hydrolyzing species. Thus, it would not be surprising for the species fraction plots multiplied by their respective rates of ATP hydrolysis to sum together in such a way that the observed total velocity, v_{obs}, could appear more or less sigmoidal depending on which species are hydrolyzing and at what relative rates. Consequently, the observation of a sigmoidal dependence alone cannot be used to conclude that there is cooperativity between nucleotide binding sites since the sigmoidal dependence illustrated in Figure 6 is entirely due to changes in the assembly state.

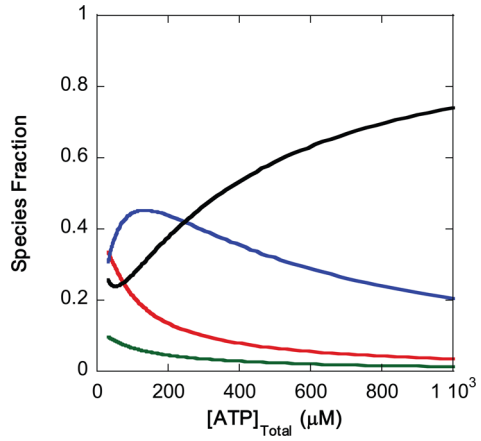

Figure 6. Species fraction plot as a function of total [ATP]. Species fractions were simulated using eqs 23−26 for a total ClpB monomer concentration of 5 μM and the parameters in Table 4 and the values for $L_{2,0}$, $L_{4,0}$, and $L_{6,0}$ in Table 1 from our previous work.[31] Solid lines are monomer (red), dimer (green), tetramer (blue), and hexamer (black).

Significance of $L_{n,0}$ and $L_{n,app}$. The significance of the self-association equilibrium constant in the absence of nucleotide, $L_{n,0}$, is that it represents the intrinsic propensity of the protein to assemble.[31] That is to say, the tendency of ClpB to form, for example, hexamers in the absence of nucleotide is governed by the chemical composition of the monomeric units. Naturally, parameters that may influence the magnitude of this parameter are the typical thermodynamic parameter: solution conditions, temperature, pressure, etc. However, any modification to the primary structure of the protein may cause there to be changes in $L_{n,0}$.

The significance of the ligand-linked assembly constant, $L_{n,app}$, is that it defines the concentration of oligomers present at a given concentration of free nucleotide and is a function of the nucleotide binding constants. Most importantly it is not constant as a function of [ATP], one of the primary substrates of interest for any ATP driven motor protein and the independent variable in a steady-state ATPase experiment. Consequently, any interpretation of an experiment performed that varies the concentration of the nucleotide substrate must incorporate the changing distribution of oligomers in solution.

Steady-state ATP hydrolysis experiments and titrations of protein with nucleotide using either ITC or fluorescence will all exhibit different distributions of states at each titration point. Equally important, the equations that have been derived to describe these types of experiments have been derived with the express assumption that the macromolecule being titrated does not change its assembly state during the course of the titration. For example, the assumptions built into the Michaelis−Menten equation,[50] the Hill equation,[51] and the *n*-independent and identical sites model built into most manufacturer's software for

DOI: 10.1021/acs.biochem.6b00122
Biochemistry 2016, 55, 1758−1771

the ITC do not apply to a system that changes its assembly state at each titration point.[52−54] Therefore, knowledge of $L_{n,app}$ is essential to be able to interpret such experiments. Further, models must be derived on a case by case basis to account for macromolecular assembly as we recently did for polypeptide binding for both ClpA and ClpB.[55,56]

Mutational analysis has been the technique of choice for many studies on ClpB and Hsp104. Typically, when a modification is made in the primary structure of the protein, gel permeation chromatography is performed in the presence of nucleotide to determine if hexamers are still formed after modification. However, the observation of hexamers alone does not reveal whether the nucleotide driven self-association equilibrium constant, $L_{n,app}$, has been perturbed. Equally important, it does not reveal if there has been an impact on the intrinsic ability of the protein to assemble, i.e., $L_{n,0}$.

$L_{n,app}$ is the product of the intrinsic propensity of the protein to assemble, $L_{n,0}$, and a term the describes nucleotide binding. Specifically, as can be seen in eq 5 it is $L_{n,0}$ multiplied by the ratio of partition functions for nucleotide binding to the oligomer, P_n, divided by the partition function for the monomer, P_1, to the nth power. Consequently, there are three ways in which an introduced mutation can impact $L_{n,app}$ and thereby the distribution of oligomers present in solution. First, as described above, it can affect the intrinsic propensity of the protein to assemble, $L_{n,0}$. Second, it can affect the nucleotide binding constant for nucleotide binding to the oligomer. Third, it can affect the nucleotide binding constant for nucleotide binding to the monomer. Thus, the observation that hexamers are still formed from a gel permeation chromatography experiment at one fixed total protein, and nucleotide concentration does not reveal the extent to which the mutation will shift the equilibrium of oligomers in subsequent activity measurements. Thus, it is entirely possible that the observation of enhanced or repressed activities upon mutation may be directly linked to perturbations in the intrinsic assembly state or the ligand linked assembly state.

Determination of the Binding Stoichiometry and Affinity of ATPγS to Each ClpB Oligomer. As shown from the analysis of the dependence of the equilibrium constants on nucleotide concentration (Figure 4 and Table 4), hexameric ClpB exhibits a maximum binding stoichiometry of 12. This observation is in direct contrast to previously published results using isothermal titration calorimetry (ITC).[57] In that work the binding isotherms were well described by the n-independent and identical sites model with $n = 1$. From that observation it was concluded that only D2 in the hexamer is capable of binding ATPγS, and thus the hexamer has a maximum stoichiometry of six nucleotides.

As noted above, it is imperative to reiterate that the derivation of the n-independent and identical sites model used in the analysis of the ITC data is derived under the express assumption that the macromolecule does not change its assembly state during the titration. To fall within the bounds of this assumption, at sufficiently high protein concentrations, it may be reasonable to assume that everything is in the hexameric state and not changing during the titration. This was the assumption invoked in Fernandez-Higuero et al. in that study when using 28 μM ClpB.[57]

To address the assumption that all of the ClpB is in the hexameric state at a total [ClpB] = 28 μM, we simulated a species fraction plot as a function of [ATP] for a fixed 28 μM total ClpB concentration, which is the protein concentration used by Fernandez-Higueor et al.[57] The simulation was done using the nucleotide binding constants and stoichiometries given in Table 4 and $L_{n,0}$ from Lin and Lucius[31] (Figure S6). Our simulations show that the fraction of hexamers drops and the fraction of tetramers increase over a mole ratio of 0−2 [ATP]/[ClpB], precisely the range over which their ITC thermogram exhibited a steep transition.

With the simulated species fractions in mind, it is possible that the enthalpy of macromolecular assembly dominates the thermogram in the ITC experiments reported by Fernandez-Higueor et al.[57] In addition to nucleotide binding, there will also be an enthalpy associated with oligomer formation or dissociation. In fact, this has been shown to be the case for *T. thermophilus* ClpB. Beinker et al. constructed isolated fragments of D1 and D2. Upon titrating the D1 fragment into the D2 fragment an enthalpy of assembly of D1 and D2 was reported to be ∼ −38.7 kcal mol^{-1}. This titration was done in the absence of nucleotide and indicates a large heat corresponding only to protein−protein interactions. In contrast, the enthalpies reported for titrating nucleotide into a sample of ClpB ranged between ∼4−13 kcal mol^{-1} suggesting that the entire thermogram could represent changes in assembly state and not nucleotide binding at all.[57]

More recently, low resolution thermograms have been reported, in a supplemental, for titrations of a high concentration of ClpB (678 μM) titrated with ADP.[29] A stoichiometry of 7.5 ± 0.1 is reported. However, the curves are clearly biphasic, the fits are not shown, and a mere 2.5−3.0-fold molar excess of nucleotide over ClpB hexamer is shown. Consequently, there was not enough nucleotide in those titrations to saturate all of the binding sites since there are 12 nucleotide binding sites per hexamer. How a stoichiometry of 7.5 ± 0.1 was extracted from these data is entirely unclear. Moreover, even at these high protein concentrations, due to the higher affinity of nucleotide for the monomer, our simulations show that the distribution of oligomeric states will still be perturbed upon addition of nucleotide and likely contribute to the observed enthalpy of reaction.

Structural Implications of Observed Stoichiometry. In contrast to monomers within a hexamer, we show that each ClpB monomer binds only one ATPγS and its binding affinity is close to 1 order of magnitude stronger than the average binding affinity for hexamers (see Table 4). Recall, there are two nucleotide binding sites per monomer. Thus, our finding suggests that only one of the nucleotide binding domains is available for ATPγS binding when there is no adjacent subunit present. These results do not reveal if the binding is to D1 or D2. However, Yamasaki et al. performed mutations in the arginine finger of the adjacent subunit of ClpB for each NBD and showed that D1 requires the arginine finger from an adjacent subunit to fully form the nucleotide binding site. In contrast, the arginine finger from the adjacent subunit is not required for D2.[58] Thus, we conclude that D2 is most likely bound by nucleotide in the monomer.

Previous studies using the isolated fragments of ClpB D1-M-domain and D2-C-terminal domain support this conclusion.[22,59,60] They have shown that both the isolated D1-M-domain and D2-C-terminal domain cannot assemble to form hexamers. Thus, binding of ATP to the individual domains can be considered to represent the binding to the individual domain in the full length monomer. They showed that the D2-C-terminal domain has nucleotide binding ability, whereas the D1-M-domain does not. This is consistent with our observation

DOI: 10.1021/acs.biochem.6b00122
Biochemistry 2016, 55, 1758−1771

that only one site can bind to ATPγS in the full length ClpB monomer.

Interestingly, the need for an adjacent monomer to complete the D1 binding is consistent with our observed stoichiometries for the intermediate assembly states. The two intermediates (dimers and tetramers) both present stoichiometries that are one fewer than the maximum, ∼3 and 7 for dimers and tetramers that have four and eight binding sites, respectively. Moreover, the hexamer exhibits a stoichiometry of 12, which is the maximum number of binding sites that would be present in a hexameric ring. This suggests that the dimer and tetramer are not closed ring structures because an open ring would leave one incomplete nucleotide binding site if adjacent arginine residues are required to complete the binding pocket. Further, the hexamer is a closed ring and presents a binding stoichiometry of 12, an observation consistent with containing all 12 fully formed binding sites.

ClpB Hexamer Dissociation Rate Constant Has an ATPγS Concentration Dependence. Previous studies reported stopped-flow FRET experiments designed to monitor the kinetic stability of ClpB oligomers.[61−63] What was termed the subunit exchange rate for ClpB hexamer was reported. In those experiments, a FRET donor-labeled ClpB sample was rapidly mixed with a FRET acceptor-labeled ClpB sample. The FRET signal change as a function of time was recorded and fitted using one or a sum of exponentials. The measured rate constants were reported to be "subunit exchange rates". However, it is important to note that the reported parameters are actually observed rate constants resulting from a combination of both dissociation and reassociation events. Consequently, the parameter will exhibit a protein and nucleotide concentration dependence. However, this concentration dependence has not been examined. Further, even though these studies have been interpreted as hexamer exchange rates, the FRET signal is also sensitive to changes in the dimer and tetramer concentrations.

Using this FRET stopped-flow assay apparent contradictions have been reported on the subunit exchange rate of ClpB in the presence of ATP.[61,62] Werbeck et al. reported that *T. thermophilus* ClpB hexamer resides in rapid subunit exchange using 0.2 μM FRET pair labeled ClpB in the presence of 200 μM ATP/ATPγS.[61] In contrast, Aguado et al. reported what they termed slow "subunit shuffling" when using 0.4 μM FRET pair labeled *E. coli* ClpB in the presence of 2 mM ATP.[62] The observed rate constant reported by Aguado et al. is 2 orders of magnitude smaller than the slowest rate constant reported by Werbeck et al. However, based on the values reported in Table 4, the conditions reported by Werbeck et al. would contain 90.8% monomer, 5.2% dimer, 3.8% tetramer, and 0.2% hexamer. In contrast, the conditions reported by Aguado et al. would contain 16% monomer, 3% dimer, 22% tetramer, and 59% hexamer. Consequently, the two studies are likely assaying an entirely different population of oligomers.

The two studies were performed using enzymes from two different organisms, and this may also contribute to the apparent discrepancy. However, the most noticeable difference that also needs to be considered, based on the results reported here, is that each study was performed at a different protein and nucleotide concentration and neither study examined the nucleotide or protein concentration dependence of the kinetic parameters.

Sedimentation velocity experiments can yield kinetic information on assembly under a limited range of dissociation rate constants.[36] However, unlike the FRET experiment that is reporting on the summation of all of the oligomers, the kinetic information acquired in the approach presented here can be assigned to a specific oligomer. Our results show that the hexamer and tetramer are in slow subunit exchange at high nucleotide concentration and fast exchange at low nucleotide concentration, while the dimer appears to be under rapid exchange at all nucleotide concentrations. Thus, when the protein and nucleotide concentration dependencies are taken into account the two FRET studies may be in complete agreement.

It has been proposed that subunit exchange is mechanistically important.[61] The idea is that during protein disaggregation dissociation of the hexamer serves as a "fail-safe". If the translocating enzyme encounters a highly stable structure it will tend to disassemble instead of continuing to translocate. Our results are disproving this model. First, we have shown that ClpB does not processively translocate.[30] Thus, if ClpB encounters a stable structure, it is more likely to dissociate due to low processivity and not stability of the hexameric ring. Second, our results in this paper, which reflect the dissociation rate constant for the isolated hexamer, reveal that at cellular concentrations of nucleotide the hexamer does not exhibit rapid dissociation. The rapid subunit exchange that was previously reported from the FRET study was likely the consequence of changing assembly states of dimers and tetramers.

Biological Significance of Ligand Linked Assembly for ClpB and Related Proteins. Beyond the clear need for the ClpB self-assembly energetics for the design and interpretation of in vitro experiments, the hexamerization equilibrium likely plays a regulatory role in vivo. Indeed, the nucleotide concentration in the cell is well above the $K_d \approx 5-30$ μM for nucleotide binding to all of the oligomers. However, the midpoint for hexamer formation (∼3 μM) as a function of protein at saturating nucleotide is near the reported 9 μM ClpB in the cell at 30 °C.[28]

If binding of the cochaperone, DnaK, to the m-domain perturbs the nucleotide ligation state, then the concentration of hexamers present and available to do mechanical work will be shifted. The reported concentration of DnaK in the cell is ∼27 μM,[28] which is nearly identical to the reported ClpB DnaK affinity of 25 μM.[18] Consequently, the cell may be able to regulate ClpB function by modulating both the DnaK and ClpB concentration. Thus, going forward, it is imperative to determine how the DnaK binding affinity is coupled to $L_{6,app}$.

The work presented here will set the stage for us to quantitatively determine how binding of partner proteins may regulate the function of ClpB. Moreover, a common theme for AAA+ molecular chaperones is nucleotide linked assembly and interaction with partner proteins. Thus, the overall strategy presented here can be broadly applied to a large number of homologous proteins where understanding the thermodynamics of the various protein−protein interactions will be essential for understanding the biological function.

■ ASSOCIATED CONTENT

Supporting Information

The Supporting Information is available free of charge on the ACS Publications website at DOI: 10.1021/acs.biochem.6b00122.

Micromath Scientist model for predicting monomer, dimer, tetramer, and hexamer concentrations as a

DOI: 10.1021/acs.biochem.6b00122
Biochemistry 2016, 55, 1758−1771

function of nucleotide concentration. Figure S1: Sedimentation velocity results on ATPγS. Figure S2: Difference curves for 2, 3, 6, and 10 μM ClpB with 200 μM ATPγS. Figure S3: Global analysis of $\log(L_{n,app})$ vs $[ATP\gamma S]_f$ assuming monomer does not bind nucleotide. Figure S4: Grid search analysis on nucleotide binding constants. Figure S5: Comparison of global analysis of $\mathrm{Log}(L_{n,app})$ vs $[ATP\gamma S]_f$ for cooperative and non-cooperative models. Figure S6: Species fraction plots for 28 μM ClpB. Equations S.1−S.3: Functional dependence of $L_{n,app}$ on nucleotide for cooperative nucleotide binding (PDF)

AUTHOR INFORMATION

Corresponding Author

*E-mail: allucius@uab.edu; phone: 205-934-8096; fax: 205-934-2543.

Funding

This work was supported by National Science Foundation (NSF) Grant MCB-1412624 to A.L.L.

Notes

The authors declare no competing financial interest.

ACKNOWLEDGMENTS

We would like to thank Dr. Walter Stafford and BBRI for the XL-I analytical ultracentrifuge. Thanks to Elizabeth Duran, Clarissa Weaver, and Nate Scull for comments on the manuscript.

ABBREVIATIONS:

AAA+, ATPase associated with various cellular activities; ATP, adenosine triphosphate; ATPγS, adenosine 5′-(γ-thio)-triphosphate; ClpB, caseinolytic peptidase B; Hsp, heat shock protein; NDB, nucleotide binding domain; NLLS, nonlinear-least-squares; RMSD, root mean squared deviation

REFERENCES

(1) Schirmer, E. C., Glover, J. R., Singer, M. A., and Lindquist, S. (1996) HSP100/Clp proteins: a common mechanism explains diverse functions. *Trends Biochem. Sci. 21*, 289−296.

(2) Arlt, H., Tauer, R., Feldmann, H., Neupert, W., and Langer, T. (1996) The YTA10−12 complex, an AAA protease with chaperone-like activity in the inner membrane of mitochondria. *Cell 85*, 875−885.

(3) Neuwald, A. F., Aravind, L., Spouge, J. L., and Koonin, E. V. (1999) AAA+: A class of chaperone-like ATPases associated with the assembly, operation, and disassembly of protein complexes. *Genome Res. 9*, 27−43.

(4) Lee, S., and Tsai, F. T. (2005) Molecular chaperones in protein quality control. *J. Biochem. Mol. Biol. 38*, 259−265.

(5) Ogura, T., and Wilkinson, A. J. (2001) AAA+ superfamily ATPases: common structure−diverse function. *Genes Cells 6*, 575−597.

(6) Vale, R. D. (2000) AAA proteins. Lords of the ring. *J. Cell Biol. 150*, F13−19.

(7) Cashikar, A. G., Schirmer, E. C., Hattendorf, D. A., Glover, J. R., Ramakrishnan, M. S., Ware, D. M., and Lindquist, S. L. (2002) Defining a pathway of communication from the C-terminal peptide binding domain to the N-terminal ATPase domain in a AAA protein. *Mol. Cell 9*, 751−760.

(8) Doyle, S. M., Shorter, J., Zolkiewski, M., Hoskins, J. R., Lindquist, S., and Wickner, S. (2007) Asymmetric deceleration of ClpB or Hsp104 ATPase activity unleashes protein-remodeling activity. *Nat. Struct. Mol. Biol. 14*, 114−122.

(9) Doyle, S. M., Hoskins, J. R., and Wickner, S. (2007) Collaboration between the ClpB AAA+ remodeling protein and the DnaK chaperone system. *Proc. Natl. Acad. Sci. U. S. A. 104*, 11138−11144.

(10) Doyle, S. M., and Wickner, S. (2009) Hsp104 and ClpB: protein disaggregating machines. *Trends Biochem. Sci. 34*, 40−48.

(11) Desantis, M. E., and Shorter, J. (2012) The elusive middle domain of Hsp104 and ClpB: location and function. *Biochim. Biophys. Acta, Mol. Cell Res. 1823*, 29−39.

(12) Goloubinoff, P., Mogk, A., Zvi, A. P., Tomoyasu, T., and Bukau, B. (1999) Sequential mechanism of solubilization and refolding of stable protein aggregates by a bichaperone network. *Proc. Natl. Acad. Sci. U. S. A. 96*, 13732−13737.

(13) Glover, J. R., and Lindquist, S. (1998) Hsp104, Hsp70, and Hsp40: a novel chaperone system that rescues previously aggregated proteins. *Cell 94*, 73−82.

(14) Shorter, J., and Lindquist, S. (2008) Hsp104, Hsp70 and Hsp40 interplay regulates formation, growth and elimination of Sup35 prions. *EMBO J. 27*, 2712−2724.

(15) Motohashi, K., Watanabe, Y., Yohda, M., and Yoshida, M. (1999) Heat-inactivated proteins are rescued by the DnaK.J-GrpE set and ClpB chaperones. *Proc. Natl. Acad. Sci. U. S. A. 96*, 7184−7189.

(16) Zolkiewski, M. (1999) ClpB cooperates with DnaK, DnaJ, and GrpE in suppressing protein aggregation. A novel multi-chaperone system from Escherichia coli. *J. Biol. Chem. 274*, 28083−28086.

(17) Lee, S., Sielaff, B., Lee, J., and Tsai, F. T. (2010) CryoEM structure of Hsp104 and its mechanistic implication for protein disaggregation. *Proc. Natl. Acad. Sci. U. S. A. 107*, 8135−8140.

(18) Rosenzweig, R., Moradi, S., Zarrine-Afsar, A., Glover, J. R., and Kay, L. E. (2013) Unraveling the mechanism of protein disaggregation through a ClpB-DnaK interaction. *Science 339*, 1080−1083.

(19) Mogk, A., Schlieker, C., Strub, C., Rist, W., Weibezahn, J., and Bukau, B. (2003) Roles of individual domains and conserved motifs of the AAA+ chaperone ClpB in oligomerization, ATP hydrolysis, and chaperone activity. *J. Biol. Chem. 278*, 17615−17624.

(20) Schlee, S., Groemping, Y., Herde, P., Seidel, R., and Reinstein, J. (2001) The chaperone function of ClpB from Thermus thermophilus depends on allosteric interactions of its two ATP-binding sites. *J. Mol. Biol. 306*, 889−899.

(21) Watanabe, Y. H., Motohashi, K., and Yoshida, M. (2002) Roles of the two ATP binding sites of ClpB from Thermus thermophilus. *J. Biol. Chem. 277*, 5804−5809.

(22) Beinker, P., Schlee, S., Auvula, R., and Reinstein, J. (2005) Biochemical coupling of the two nucleotide binding domains of ClpB: covalent linkage is not a prerequisite for chaperone activity. *J. Biol. Chem. 280*, 37965−37973.

(23) Hattendorf, D. A., and Lindquist, S. L. (2002) Cooperative kinetics of both Hsp104 ATPase domains and interdomain communication revealed by AAA sensor-1 mutants. *EMBO J. 21*, 12−21.

(24) Lee, S., Sowa, M. E., Watanabe, Y. H., Sigler, P. B., Chiu, W., Yoshida, M., and Tsai, F. T. (2003) The structure of ClpB: a molecular chaperone that rescues proteins from an aggregated state. *Cell 115*, 229−240.

(25) Schirmer, E. C., Ware, D. M., Queitsch, C., Kowal, A. S., and Lindquist, S. L. (2001) Subunit interactions influence the biochemical and biological properties of Hsp104. *Proc. Natl. Acad. Sci. U. S. A. 98*, 914−919.

(26) Alberty, R. A. (1969) Standard Gibbs free energy, enthalpy, and entropy changes as a function of pH and pMg for several reactions involving adenosine phosphates. *J. Biol. Chem. 244*, 3290−3302.

(27) Simmons, R. M., and Hill, T. L. (1976) Definitions of free energy levels in biochemical reactions. *Nature 263*, 615−618.

(28) Mogk, A., Tomoyasu, T., Goloubinoff, P., Rudiger, S., Roder, D., Langen, H., and Bukau, B. (1999) Identification of thermolabile Escherichia coli proteins: prevention and reversion of aggregation by DnaK and ClpB. *EMBO J. 18*, 6934−6949.

(29) Carroni, M., Kummer, E., Oguchi, Y., Wendler, P., Clare, D. K., Sinning, I., Kopp, J., Mogk, A., Bukau, B., and Saibil, H. R. (2014) Head-to-tail interactions of the coiled-coil domains regulate ClpB

DOI: 10.1021/acs.biochem.6b00122
Biochemistry 2016, 55, 1758−1771

activity and cooperation with Hsp70 in protein disaggregation. *eLife 3*, e02481.
(30) Li, T., Weaver, C. L., Lin, J., Duran, E. C., Miller, J. M., and Lucius, A. L. (2015) Escherichia coli ClpB is a non-processive polypeptide translocase. *Biochem. J. 470*, 39−52.
(31) Lin, J., and Lucius, A. L. (2015) Examination of the dynamic assembly equilibrium for E. coli ClpB. *Proteins: Struct., Funct., Genet. 83*, 2008−2024.
(32) Zhao, H., Ghirlando, R., Piszczek, G., Curth, U., Brautigam, C. A., and Schuck, P. (2013) Recorded scan times can limit the accuracy of sedimentation coefficients in analytical ultracentrifugation. *Anal. Biochem. 437*, 104−108.
(33) Schuck, P. (1998) Sedimentation analysis of noninteracting and self-associating solutes using numerical solutions to the Lamm equation. *Biophys. J. 75*, 1503−1512.
(34) Stafford, W. F., and Sherwood, P. J. (2004) Analysis of heterologous interacting systems by sedimentation velocity: curve fitting algorithms for estimation of sedimentation coefficients, equilibrium and kinetic constants. *Biophys. Chem. 108*, 231−243.
(35) Ortega, A., Amoros, D., and Garcia de la Torre, J. (2011) Prediction of hydrodynamic and other solution properties of rigid proteins from atomic- and residue-level models. *Biophys. J. 101*, 892−898.
(36) Lin, J., and Lucius, A. L. (2015) Analysis of Linked Equilibria. *Methods Enzymol. 562*, 161−186.
(37) Wyman, J., and Gill, S. J. (1990) *Binding and Linkage: Functional Chemistry of Biological Macromolecules*; University Science Books: Mill Valley, CA.
(38) Wyman, J., Jr. (1964) Linked Functions and Reciprocal Effects in Hemoglobin: A Second Look. *Adv. Protein Chem. 19*, 223−286.
(39) Na, G. C., and Timasheff, S. N. (1985) Velocity sedimentation study of ligand-induced protein self-association. *Methods Enzymol. 117*, 459−495.
(40) Bujalowski, W., and Lohman, T. M. (1991) Monomer-tetramer equilibrium of the *Escherichia coli* ssb-1 mutant single strand binding protein. *J. Biol. Chem. 266*, 1616−1626.
(41) Turgay, K., Hamoen, L. W., Venema, G., and Dubnau, D. (1997) Biochemical characterization of a molecular switch involving the heat shock protein ClpC, which controls the activity of ComK, the competence transcription factor of Bacillus subtilis. *Genes Dev. 11*, 119−128.
(42) Parsell, D. A., Kowal, A. S., Singer, M. A., and Lindquist, S. (1994) Protein disaggregation mediated by heat-shock protein Hsp104. *Nature 372*, 475−478.
(43) Yu, R. C., Jahn, R., and Brunger, A. T. (1999) NSF N-terminal domain crystal structure: models of NSF function. *Mol. Cell 4*, 97−107.
(44) Meyer, H., and Weihl, C. C. (2014) The VCP/p97 system at a glance: connecting cellular function to disease pathogenesis. *J. Cell Sci. 127*, 3877−3883.
(45) Katayama, Y., Gottesman, S., Pumphrey, J., Rudikoff, S., Clark, W. P., and Maurizi, M. R. (1988) The two-component, ATP-dependent Clp protease of *Escherichia coli*. Purification, cloning, and mutational analysis of the ATP-binding component. *J. Biol. Chem. 263*, 15226−15236.
(46) Gottesman, S., Clark, W. P., de Crecy-Lagard, V., and Maurizi, M. R. (1993) ClpX, an alternative subunit for the ATP-dependent Clp protease of Escherichia coli. Sequence and in vivo activities. *J. Biol. Chem. 268*, 22618−22626.
(47) Rajendar, B., and Lucius, A. L. (2010) Molecular mechanism of polypeptide translocation catalyzed by the Escherichia coli ClpA protein translocase. *J. Mol. Biol. 399*, 665−679.
(48) Veronese, P. K., Rajendar, B., and Lucius, A. L. (2011) Activity of Escherichia coli ClpA Bound by Nucleoside Di- and Triphosphates. *J. Mol. Biol. 409*, 333−347.
(49) Miller, J. M., Lin, J., Li, T., and Lucius, A. L. (2013) E. coli ClpA Catalyzed Polypeptide Translocation is Allosterically Controlled by the Protease ClpP. *J. Mol. Biol. 425*, 2795−2812.
(50) Johnson, K. A., and Goody, R. S. (2011) The original Michaelis constant: translation of the 1913 Michaelis-Menten paper. *Biochemistry 50*, 8264−8269.
(51) Hill, A. V. (1913) The Combinations of Haemoglobin with Oxygen and with Carbon Monoxide. I. *Biochem. J. 7*, 471−480.
(52) Fisher, H. F., and Singh, N. (1995) Calorimetric methods for interpreting protein-ligand interactions. *Methods Enzymol. 259*, 194−221.
(53) Wiseman, T., Williston, S., Brandts, J. F., and Lin, L. N. (1989) Rapid measurement of binding constants and heats of binding using a new titration calorimeter. *Anal. Biochem. 179*, 131−137.
(54) Breslauer, K. J., Freire, E., and Straume, M. (1992) Calorimetry: a tool for DNA and ligand-DNA studies. *Methods Enzymol. 211*, 533−567.
(55) Li, T., Lin, J., and Lucius, A. L. (2015) Examination of polypeptide substrate specificity for Escherichia coli ClpB. *Proteins: Struct., Funct., Genet. 83*, 117−134.
(56) Li, T., and Lucius, A. L. (2013) Examination of Polypeptide Substrate Specificity for E. coli ClpA. *Biochemistry 52*, 4941−4954.
(57) Fernandez-Higuero, J. A., Acebron, S. P., Taneva, S. G., Del Castillo, U., Moro, F., and Muga, A. (2011) Allosteric communication between the nucleotide binding domains of caseinolytic peptidase B. *J. Biol. Chem. 286*, 25547−25555.
(58) Yamasaki, T., Nakazaki, Y., Yoshida, M., and Watanabe, Y. H. (2011) Roles of conserved arginines in ATP-binding domains of AAA + chaperone ClpB from Thermus thermophilus. *FEBS J. 278*, 2395−2403.
(59) Werbeck, N. D., Kellner, J. N., Barends, T. R., and Reinstein, J. (2009) Nucleotide binding and allosteric modulation of the second AAA+ domain of ClpB probed by transient kinetic studies. *Biochemistry 48*, 7240−7250.
(60) Werbeck, N. D., Zeymer, C., Kellner, J. N., and Reinstein, J. (2011) Coupling of oligomerization and nucleotide binding in the AAA+ chaperone ClpB. *Biochemistry 50*, 899−909.
(61) Werbeck, N. D., Schlee, S., and Reinstein, J. (2008) Coupling and dynamics of subunits in the hexameric AAA+ chaperone ClpB. *J. Mol. Biol. 378*, 178−190.
(62) Aguado, A., Fernandez-Higuero, J. A., Cabrera, Y., Moro, F., and Muga, A. (2015) ClpB dynamics is driven by its ATPase cycle and regulated by the DnaK system and substrate proteins. *Biochem. J. 466*, 561−570.
(63) DeSantis, M. E., Leung, E. H., Sweeny, E. A., Jackrel, M. E., Cushman-Nick, M., Neuhaus-Follini, A., Vashist, S., Sochor, M. A., Knight, M. N., and Shorter, J. (2012) Operational plasticity enables hsp104 to disaggregate diverse amyloid and nonamyloid clients. *Cell 151*, 778−793.

DOI: 10.1021/acs.biochem.6b00122
Biochemistry 2016, 55, 1758−1771